EVALUATION OF MICROSTRUCTURE AND MECHANICAL PROPERTIES OF TiO_2 REINFORCED ALUMINIUM COMPOSITES DEVELOPED THROUGH MULTI-STEP STIR CASTING

John Samson Khalkho, Suresh Vidyasagar Chevuri, and Benny Karunakar Dagarapu
Department of Mechanical and Industrial Engineering, Indian Institute of Technology Roorkee, Roorkee 247667, India

https://doi.org/10.1007/s40962-022-00760-6

Abstract

The present paper investigates the effect of TiO_2 particles on the microstructure and mechanical properties of AA2014 composites. AA2014 composite samples reinforced with varying amounts of TiO_2 in the range of 1–4 wt% to matrix were developed through multi-step stir casting. The mechanical properties of the developed composites and their corresponding microstructures were correlated. The microstructures revealed that TiO_2 has promoted grain refinement from dendritic to globular grains through nucleation across the AA2014 matrix due to high rate of solidification which increased with an increase in the TiO_2 content. The TiO_2 reacted with Al to form Al_2O_3 in the matrix besides Al_2CuMg, Al_2Cu secondary phases which provided additional strength to the composites. The composite sample reinforced with 4 wt% TiO_2 exhibited the best combination of mechanical properties. However, improvement in the mechanical properties beyond 3 wt% TiO_2 addition was not significant.

Keywords: *aluminium composites, multi-step stir casting, microstructure, grain refinement, phase transformation*

Introduction

There is a rapid demand for advanced materials that can sustain their critical properties in extreme conditions. Conventional monolithic materials have reached their limits in structural applications that require materials having different combinations of properties like hardness-ductility, high strength-low density, stiffness-high temperature strength, toughness-creep, wear, high corrosion resistance, etc.[1] Therefore, new generation materials with these properties are quickly replacing conventional materials. In this regard, many smart materials, composites, super-alloys, high entropy alloys, quantum nano-materials, etc., have come into focus.[2] Lightweight composites with aluminium as matrix materials have found applications in various industries as a replacement to steel and other denser materials.[3] The key benefit of using aluminium alloys lies in the fact that several mechanical and tribological properties could be tailored by more than sixty percent by adding suitable reinforcements in an appropriate fraction.[4,5] Over the years, Aluminium Matrix Composites (AMCs) have been tried, modified and developed for various structural non-structural applications in various sectors such as aerospace, marine, defense and automobile.[6] These AMCs have been developed by reinforcing various materials such as metals, Rare Earth (RE),[7–10] ceramics,[11] non-metal such as graphene,[12] Carbon Nano-Tubes (CNT)[13] and Fly-Ash (FA).[14] These reinforcements may be in the form of fibres, whiskers, particulates, chips, tubes, etc.[15–17] On the other hand, AMCs have also been developed through in situ processing. For example, Zamani et al.[18] developed Al-Mg_2Si composite through in situ which exhibited a 40% increase in the UTS along with a remarkable 333% increase in the elongation as compared to base alloy. Similarly, Ayar et al.[19] achieved 64% and 50% increase in the UTS and hardness, respectively, in $AlSi_5Cu_3/TiB_2$ composite through in situ method and Senthil et al.[20] improved the corrosion resistance of Al/TiB_2 composites through the same method.

Received: 29 March 2021 / Accepted: 03 January 2022 /
Published online: 22 February 2022

Among the various ceramics reinforced to AMCs, the most common are Carbides,[21] Nitrides,[22] Borides,[23] Oxides,[24] etc. Among the oxides, Titanium Oxide (TiO_2) particles are considered to be an attractive reinforcing material due to their low cost and the ability to improve the properties of the resulting composite in which it is reinforced. Properties such as high-temperature mechanical properties, wear resistance and oxidation resistance could be effectively enhanced by reinforcing TiO_2.[25] Furthermore, TiO_2 is stable in a thermal environment and with the influence of reducing agents, it loses its oxygen only after a temperature of a few hundred degrees Celsius.[26] Oxides have been extensively used by researchers throughout the world and based on the literature, some relevant studies are reported here. Dutta et al.,[27] investigated the impact of alumina particulate reinforcement on the precipitation of as-cast AA2014. Siddesha, et al.,[28] developed AA2024/TiO_2 composites and studied the effect of variation in TiO_2 reinforcement in the range of 2–8 wt%). Their results reveal that the tensile strength, hardness and impact strength of the composites increased by 63%, 84.3% and 22.2%, respectively, with the addition of TiO_2. Nagaral et al.,[29] developed AA2014-nano-ZrO_2 composites by multi-step stir casting route with varying amounts of particulates in the range of 2–6 wt% to investigate their mechanical properties and wear performance. Their study has shown that with an increase in the addition of particulate up to 6%, the UTS, YS and hardness have increased to 30.6%, 73.02% and 69.8%, respectively.

Further, due to the high surface tension of the molten metal and low surface energies of the reinforcement particles, they tend to float on the melt surface showing poor wettability. Another problem encountered in the metal casting process is the settling of reinforcement particles' and non-uniform distribution. This is due to the difference in the densities of the reinforcement particles and the metal matrix alloy by which the particles will try to sink or float causing clustering agglomeration.[30] Kumar et al.[20] showed that the pouring temperature after stir casting affects the corrosion rate of A365 and its mechanical properties.[31] Aybarc et al.[31] developed a hybrid stir casting process. Asthari et al.[32] used a tilting method of pouring for controlled diffusion solidification of the melt to avoid dendritic structure. On the other hand, thixo casting is a method of casting aluminium in which the metal is forced into a mold in a semi-solid state to form near-net-shape components.[33] Zhou et al.[34] used high-pressure semi-solid casting to produce thin-walled components after the melt was stirred. Prapasajchavet et al.[30] plastically deformed the semi-solid mixture to obtain globular grains in the matrix. Moreover, distributing the reinforcement in the matrix in its semi-solid state through multi-step stirring could yield interesting results. However, controlling the temperature to maintain the semi-solid state is very challenging.

Therefore, this present work aims to develop AA2014 matrix composites reinforced with micro-sized TiO_2 particles in the range of 1–4 wt% through multi-step stir casting. The AA2014 is a wrought alloy with high levels of Si and Fe. While this might be fine for the production of MMC's for wrought applications, it is problematic for the production of shaped casting using MMC's. The issues are hot tears, segregation, feeding, need for solidification control, etc. However, AA2014 is widely used in larger and simpler shapes.[35] Therefore, in this study to minimize the aforementioned problems, the semi-solid slurry is reinforced with TiO2 in instalments and stirred for in the same state to attain uniform distribution. Billets are produced by leaving the melt in the crucible followed by quenching to give the billet the shape of the crucible. This billet needs further processing for obtaining the final shape and finishing as required for producing various composites. For example, as discussed above some were successful in developing AA2014 composites through various modified casting methods with various reinforcements and shapes such as ingots of different standard shapes and sizes[35] cylindrical billets,[36] square billets[37] which can be further rolled, extruded, machined into required shapes.[35] However, stirring the semisolid composite slurry in instalments without extrusion may help in avoiding casting related problems, especially associated with AA2014 composites.

Material Methods

In the present study, micro-sized TiO_2 is chosen as reinforcement and AA2014 ingot is used as the matrix. The AA2014 ingots were procured from Ampco Metal India. Pvt. Ltd. And the TiO_2 powder with 99.96% purity average particle size of 10 μm were procured from Alfa Aesar, USA. The chemical composition determined by ICPMS of the as-received AA2014 ingot is given in Table 1.

The as-received ingots are cut into pieces weighing 500 grams each. The 500 grams' chunks are further cut into smaller pieces for suitably placing them in the crucible inside the furnace. The melting temperature for the

Table 1. Chemical Composition of the As-Received AA2014 Ingot

Element	Cu	Si	Mg	Zn	Fe	Ti	Sn	Mn	Al
wt%	4.2–5	0.1	0.8	0.1	0.1	0.15–0.3	0.05	0.2–0.5	Balance

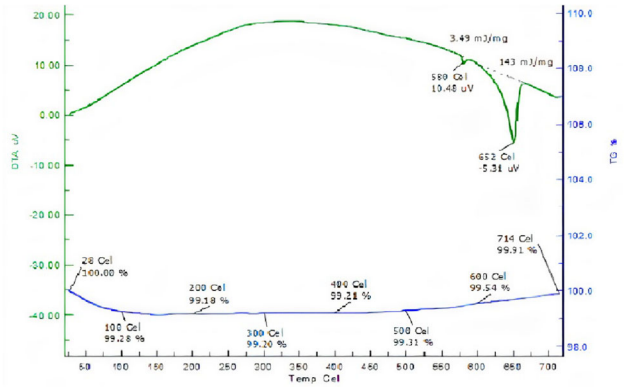

Figure 1. DTA results of AA2014 showing the melting point.

AA2014 composition used was determined to be (652 °C) by DTA as shown in Figure 1 and the melt then cooled below 600 °C, which is 50 °C below the liquidus to produce a semi-solid state.

Once all the pieces are liquefied, the reinforcement content is added to the matrix in four equal portions in four cycles. The experimental procedure is shown in Figure 2.

The TiO_2 particles preheated at 300 °C are wrapped in a thin aluminium foil and gradually added to the melt in the crucible. Arys et al.[19] developed a stir casting set-up to cast large quantities of alloys. Similarly, in the present study, a stir casting set-up was designed to cast small amounts. The mechanical stirring is then introduced into the melt and continued for 5 minutes at 100 RPM for each cycle. The stirring parameters are chosen based on similar studies done by us previously.[38] A low RPM was selected as the crucible was not completely fixed in the furnace set-up, increase in the stirring speed may cause the crucible to fall inside the furnace and also the reinforcement might stick to the surface of the crucible.[39]

A graphite stirrer with three blades which was connected to a steel rod was used for stirring and a digital meter resistor is used to monitor and control the temperature and speed. The first portion of reinforcement is added and stirred. The

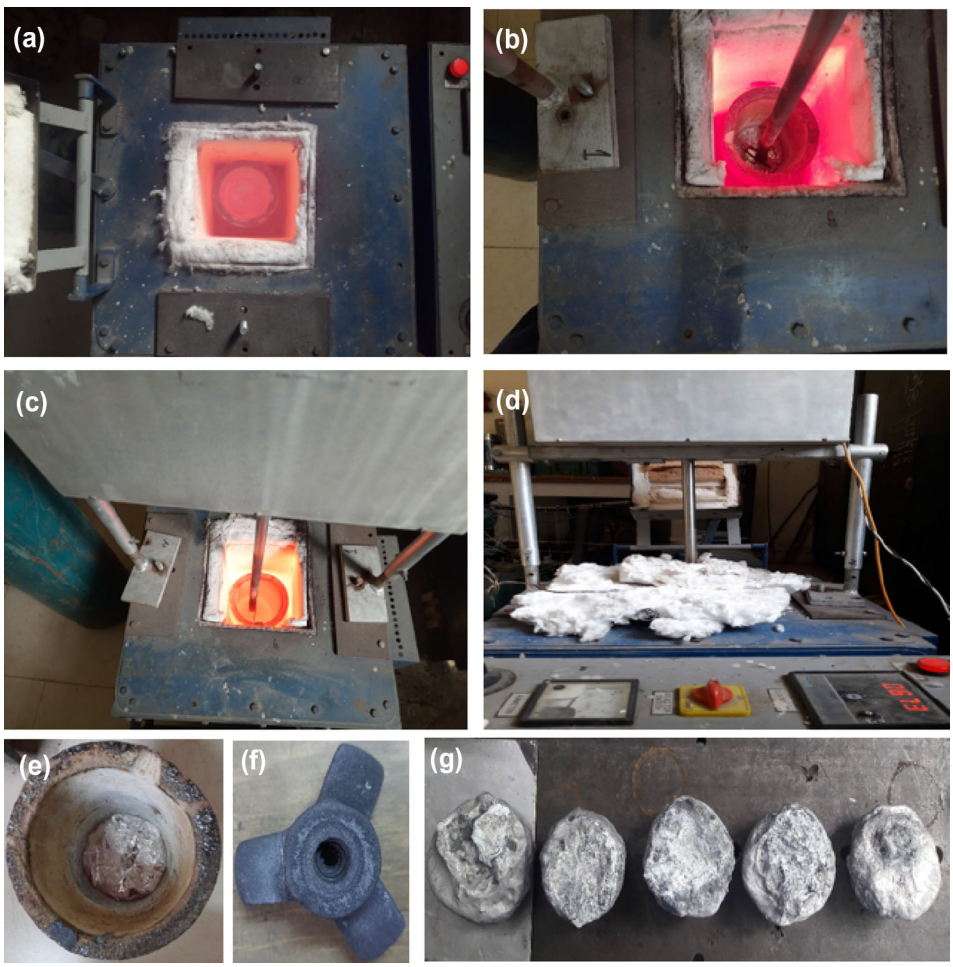

Figure 2. Experimental design (a) Molten metal in the furnace, (b) Semi-solid state stirring, (c) Liquid state stirring, (d) Custom designed stir casting set-up, (e) Solidified cast in the crucible, (f) Graphite stirrer and (g) Cast samples.

Table 2. Relative Density, Grain Size, and Mechanical Properties

TiO_2 wt%	Relative density %	Grain size	Hardness (Hv)	UTS (Mpa)	YS (Mpa)	Elongation %	Compressive strength (Mpa)
0	96.23	180	57±2.4	172±14	135±9	19.6±1.2	472±22
1	97.91	46	72.83±3.6	211±19	179±8	17.4±1.9	629±31
2	98.24	43	81.67±3.2	277±14	244±11	16.1±2.4	733±16
3	98.60	32	88.18±4.7	308±12	279±10	14.9±2.8	786±19
4	98.54	30	91.16±1.9	318±08	302±7	12.9±1.5	793±18

molten metal is then allowed to cool again until it becomes semi-solid below 600 °C, and the viscosity of the semi-solid melt increases gradually upon stirring physical observation). In the semi-solid state, the reinforcement particles get mixed up uniformly (like a dough).[39] Then the semisolid slurry is then reheated to above liquidus temperature for the slurry to reach liquid state again. Now, the second portion of reinforcement particles is added into the melt and mechanical stirring is performed. This procedure is followed for four cycles. The percentages of solid–liquid were not calculated; however, from the literature, it is found that 23% volume of liquid phase exists at 632 °C.[40] The temperature was monitored through a thermocouple which is placed at the centre of the furnace and controlled through a custom made resistance set-up. In the last cycle, a degassing agent Hexachloroethane is added to the final molten melt to remove the gases and microbubbles caused by stirring to avoid porosity. Then the crucible is removed from the furnace, and the crucible is quenched with cold water in semi-solid state. The developed samples are cut into convenient pieces for mechanical and metallurgical characterizations.

Results Discussions

In this work, a multi-step stir casting method has been used to develop the composite samples with varying wt% of TiO_2. The developed composites samples were prepared further for various testing like physical, metallurgical and mechanical to evaluate and understand the mechanisms corresponding to the properties. The microstructures are shown by both optical microstructure and SEM to better define the strengthening mechanisms acting in the composites and the microstructures are related to the corresponding mechanical properties. The results of these testing are presented below.

Density

Each composite was cut into 1x1x1 cm samples to maintain uniformity. The experimental density is measured by using the Archimedean principle by measuring the weight of the sample in the air and water, respectively.[41] Both the sample preparation and testing are done according to ASTM standards. The average value is considered for further calculations. Similarly, the theoretical density of each composite is measured by using the rule of the mixture's law. After calculating the theoretical and experimental densities, the relative density of each composite sample is further calculated and presented in Table 2. It is observed that the relative density of the composite samples increased with an increase in the TiO_2 content. It is well known that this variation in the relative density directly affects the mechanical properties of the composites. The improvement in the relative density could be attributed to many factors and are discussed below. On the other hand, the theoretical density also increased resulting in an overall improvement in the relative density of the composites. From Table 2, it is observed that the Relative Density (RD) of the unreinforced sample is 96.23% and has increased to as much as 98.6% with 3 wt% TiO_2 addition and stabilized thereof at 98.54%. The RD achieved in the present study is close to that of Al composites developed through powder metallurgy[17] and comparatively higher to similar aluminium composites developed through stir casting (94–97.2%) which exhibited higher mechanical properties in the respective studies.[42,43] The improvement in the RD with the addition of TiO_2 can be attributed to the following:

1. Formation of secondary phases and their uniform distribution
2. Increasing the wettability of the reinforcement by multi-step stirring
3. Slow stirring to eliminate stirring induced bubbles
4. Addition of degassing agent.

Moreover, due to repetitive stirring for a short time in fixed intervals helps to break the gas layers and allows more metal to surround the surface of the reinforced particles. It also decreases the surface tension of melt and helps the particles to facilitate easier wetting by mixing particulates in the melt.[44,45] Besides, the reason for the composites not achieving full density can be attributed to the handling errors caused during experimentation. However, the density of all composite samples achieved is well above 96.5% due to multi-step processing.

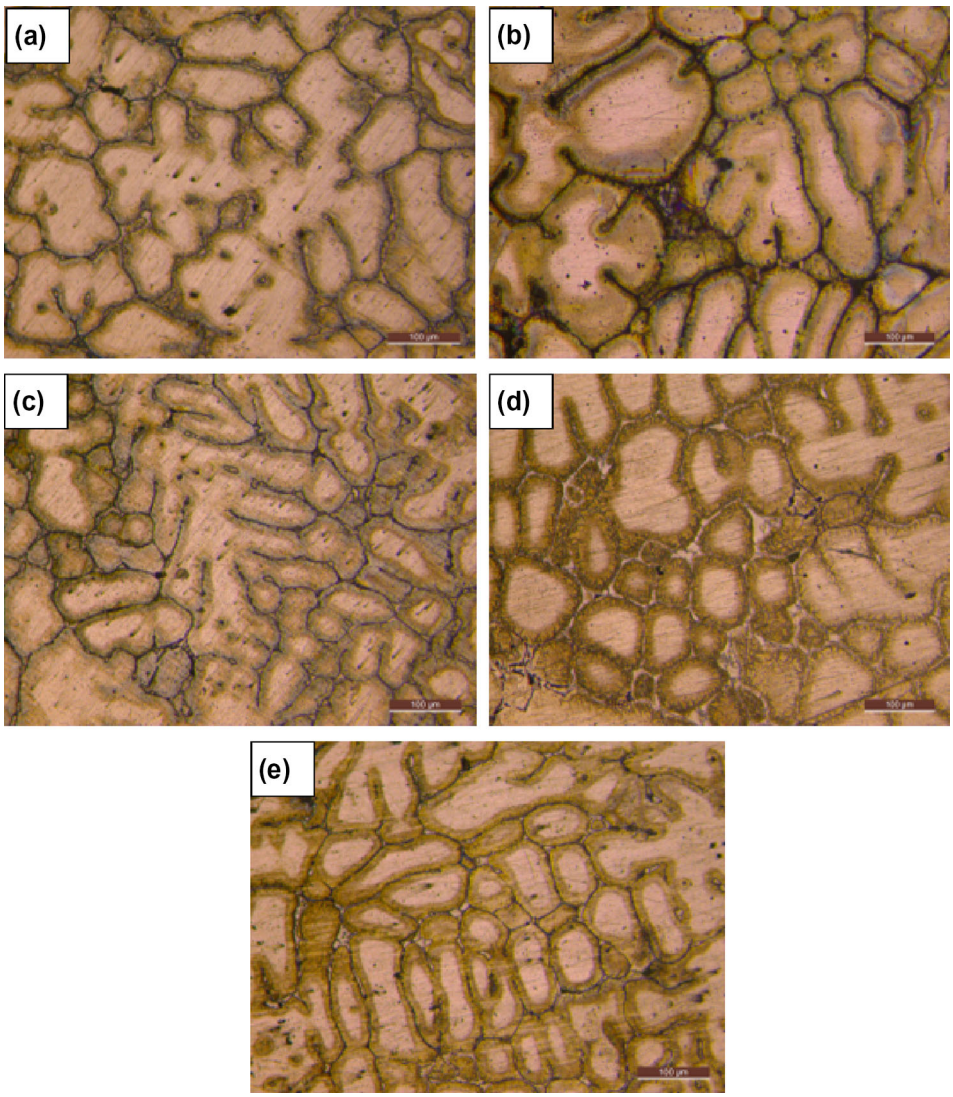

Figure 3. Optical microstructures of the composite samples reinforced with TiO_2 (a) 0.0 wt%, (b) 1 wt%, (c) 2 wt%, (d) 3 wt% (e) 4 wt%.

Microstructure Characterization

The Optical microstructures of the developed composites are shown in Figure 3. Both the sample preparation and testing are done according to ASTM standards. Figure 1(a) refers to the microstructure of as-cast AA2014. The microstructures are mainly comprised of a typical cast Dendritic Arm Structure (DAS) formed due to the high rate of cooling during solidification caused by quenching. The dendritic arms tend to become thinner and form into new grains with the addition of TiO_2 particles. However, the dendritic structure refinement is not very significant beyond 3 wt% TiO_2 addition as seen from Figure 1(b–e). The DAS manifest elongated α-Al dendrite arms covered with Al_2CuMg and Al_2Cu phases formed due to the constituents present in AA2014.

The multi-step casting and addition of TiO_2 particles have changed the solidification pattern and resulted in the dissipation of the dendrite structure of the as-cast AA2014. As the weight percentage of TiO_2 particles increased, grain refinement increased. The grain refinement suppressed the growth of α-Al as the TiO_2 particles restrict the grain size during the solidification process.[46] It is observed from the microstructures in Figure 3(b–e) that the grain size of the AA2014/TiO_2 composite reduces as the TiO_2 content increases up to 3 wt% due to an increase in the nucleation sites. However, beyond 3 wt% of TiO_2 addition, there is no significant grain refinement. An increase in the hardness and tensile strength of the composites can partly be attributed to grain refinement.

To gain further clarity on the grain refinement and secondary phases, the samples have been examined through FE-SEM. The FE-SEM microstructures of AA2014 composites reinforced with 1–4 wt% TiO_2 are shown in Figure 4. The SEM was equipped with EDAX for identifying various phases and other constituents in the composites.

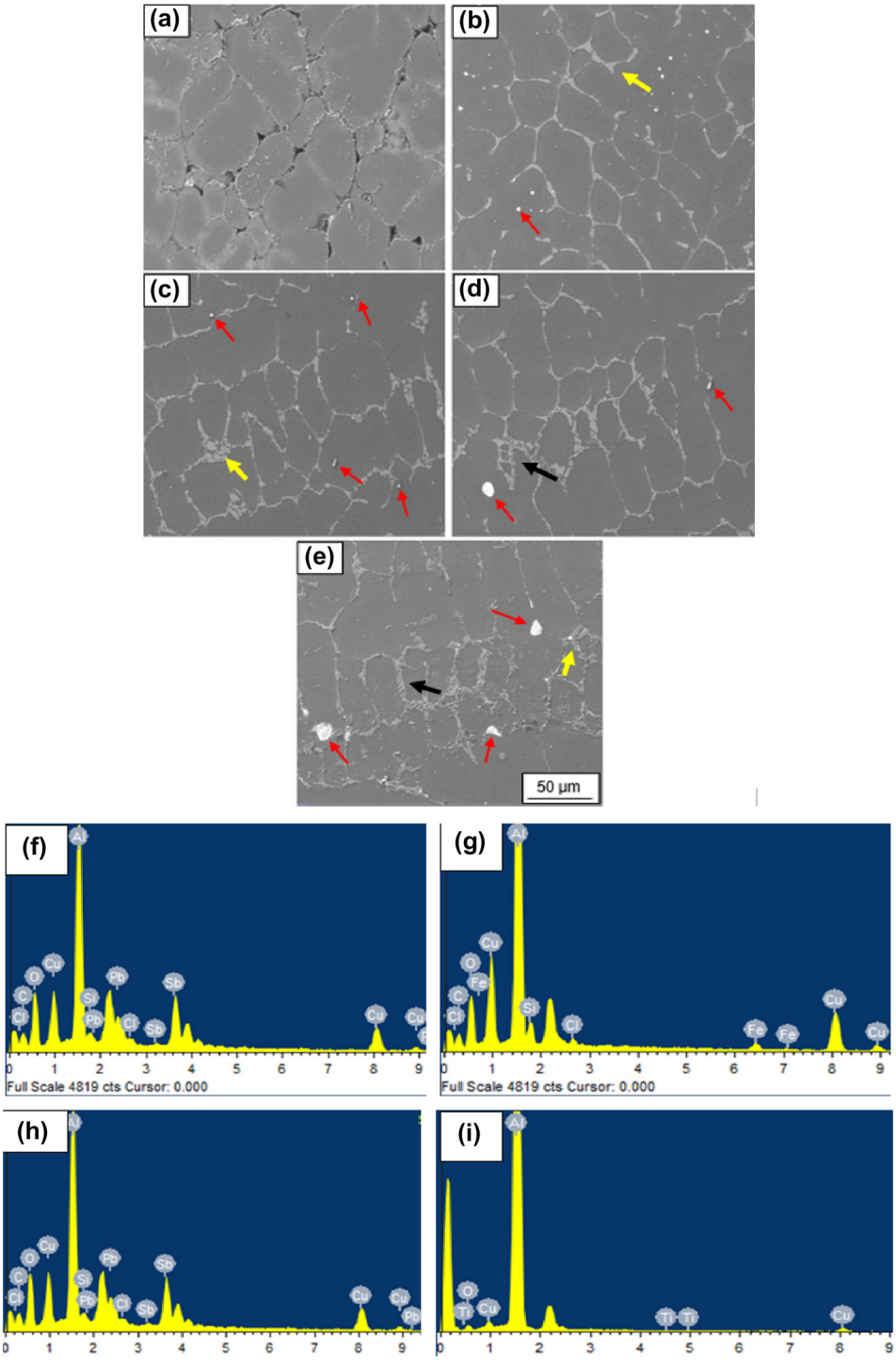

Figure 4. FE-SEM microstructures of the composite samples reinforced with TiO_2 (a) 0.0 wt%, (b) 1 wt%, (c) 2 wt%, (d) 3 wt% (e) 4 wt% EDAX of different phases present (f) Matrix, (g) Al-Cu (Black Arrows), (h) Al_2O_3 (Yellow Arrows) and (i) TiO_2 (Red Arrows).

The microstructures reveal a fine interface and good interfacial bonding between the TiO_2 particle and Al matrix. The interfacial bonding is highly desired to bear and transfer the applied load to the particles for better mechanical and tribological properties. The interfacial bonding achieved is mainly due to proper wetting of TiO_2 which is a result of the stirring method and its parameters.[47] Besides, TiO_2 particles agglomerate to form into bigger particles as their content increases as pointed out with red arrows in Figure 4 (d) (e). A clear trend of grain refinement is observed up to 3 wt% addition of TiO_2. The secondary phase around the grain boundaries increases

with an increase in the TiO_2 content. However, beyond 3 wt% addition of TiO_2, the secondary phases become coarser and no significant refinement was observed. Since the process used for this study is multi-step stirring, it improves the wetting and removes the agglomeration of reinforced particles[48] and scatters the particulates uniformly in the melt. Further, the homogeneous distribution of TiO_2 particles in the melt is influenced by the solid-state mixing used in the present study and the density variation of the TiO_2 and Al matrix. As the stirring is done in multi-steps, the gas layers on the particles are instantly broken, which increases the wetting angle, and thus, the clustering of particles and shrinkage is reduced.[49] The differences in the densities of the TiO_2 Al matrix also play a role in the distribution of TiO_2 in the matrix. The reinforced particles may not sink immediately after injecting into the semi-solid melt. The semi-solid state was identified based on temperature and observation. However, the pressure difference induced by the vortex works as an acting force to get the particle deep into melt across the radius of a vortex.

The back-scattering technique through FE-SEM is used to focus on the secondary phases formed in the matrix during casting. Figure 5 shows the back-scattered microstructures of the developed composites.

The constituent elements present in AA2014 that are higher than their solubility limit are mainly Cu and Mg. Because of this reason, some phases such as Al_2O_3, Al_2CuMg and Al_2Cu are formed around the dendrites during casting as marked in Figure 5. However, any phase involving Ti was not identified as such in the matrix, despite its presence. In Figure 5, the secondary phase Al_2Cu is marked in blue circles, Al_2CuMg intermetallic is marked in red circles and the Al_2O_3 formation is pointed out with red arrows. These phases are still present when the dendrite structure has been gradually refined into intergranular. It is well known that aluminium is prone to quick oxidation as TiO_2 is added into the melt, the aluminium readily reacts with the oxide present in TiO_2 to form Al_2O_3 which is also observed in the microstructures. Another intermetallic in the form of a Chinese script is also observed in the matrix which coarsened beyond 3 wt% TiO_2 addition along with Al_2Cu as seen from Figure 5(d). The formation of oxides other phases in the matrix provides additional strength apart from the dispersion strengthening provided by the TiO_2 particles.

XRD Analysis

In the present work, XRD analysis is done to investigate various phases and compounds at the interface of the matrix and the reinforcement of the composite. The XRD D8 Advance, Bruker AXS, USA equipment is used for XRD analysis. The XRD analysis is carried out using Cu anode at an angle (2θ) ranging from 20°–80°, the scan speed of 0.5°/m step size of 0.1° is used. The phase identification analysis is done by 'Xpert High score software'. Both the sample preparation and testing are done according to ASTM standards. The XRD patterns of the developed composites are shown in Figure 6. The figure reveals different diffraction peaks related to precipitation and intermetallic phases formed due to the interaction between α-Al

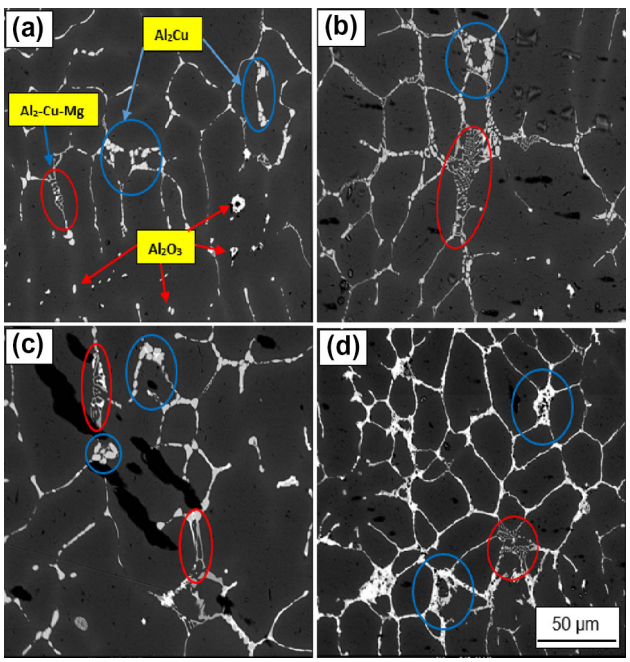

Figure 5. SEM microstructures of AA2014 composites reinforced with TiO_2 (a) 1 wt% (b) 2 wt% (c) 3 wt% (d) 4 wt%.

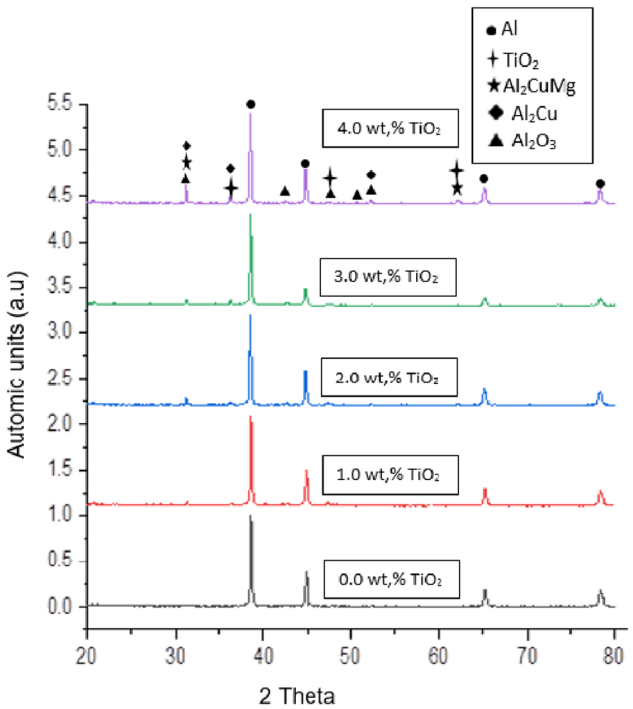

Figure 6. XRD patterns of the developed composites.

TiO_2. Five diffraction peaks of α-Al, TIO_2, Al_2O_3, Al_2Cu and Al_2CuMg phases are identified from the XRD patterns. The peak intensities of Al_2O_3 and Al_2Cu increase with an increase in the TiO_2 wt%. From Figure 6, it is noticed that any other compound such as Al_3Ti is not identified.

Mechanical Properties

The developed composite samples are further prepared for mechanical testing. Both the sample preparation and testings are done according to ASTM standards. The mechanical properties such as micro-hardness, tensile strength, ductility and compressive strength are found through testing for evaluating the effect of TiO_2 reinforcement. The relative density and the mechanical properties of the developed composites are shown in Table 2.

Microhardness

The microhardness of the developed composite samples is evaluated using a computerized Vickers hardness testing machine (Model: FIE VM 50 PC). Each composite sample is prepared for microhardness testing by polishing it to a mirror finish. The indentation on the polished surfaces of the composite is done by a diamond point indenter with a load of 100 grams for a dwell time of 10 seconds each. Ten microhardness readings are taken on the sample and the average values are reported with error bars showing maximum and minimum values. Both the sample preparation testing is done according to ASTM E-92 standards. It is observed that the microhardness of the composites gradually increased with an increase in the content of TiO_2 addition. The composite sample with 4 wt% of TiO_2 particulate exhibited a maximum hardness of 91 HV which is 74% higher compared to that of the unreinforced AA2014 sample. The hardness of TiO_2 particles is very high as compared to AA2014 which improves its resistance to plastic deformation and hence increases the hardness. The other factor that contributes to hardness is the grain size reduction which leads to more grain boundaries.[50] The TiO_2 particles act as nucleating agents and create heterogeneous nucleation in the matrix.[51] Therefore, with an increase in the wt% of TiO_2, nucleation sites increase resulting in refinement of matrix microstructure. More the grain refinement, the more grain boundaries it produces. These grain boundaries act as an obstacle to the slip planes' and increases the hardness according to the Hall-Petch relation.[52]

Also, thermal stresses are induced in the matrix due to the difference in the coefficient of thermal expansion of the matrix (AA2014) (23×10^{-6}/k) and reinforcement TiO_2 (11.8×10^{-6}/k). These thermal stresses result in the generation of dislocation at the AA2014/TiO_2 interface after solidification. As the wt% of TiO_2 content increases, it gives rise to increased dislocation density in the composite and thus improves the hardness.

Tensile Strength and Elongation

Tensile testing of the developed composites was performed to evaluate the tensile strength, yield strength and percentage elongation at fracture. Three cylindrical tensile specimens were prepared according to ASTM E08-8 standard from each developed composite and the average values are presented with error bars representing maximum and minimum. The testing is conducted on a Universal Testing Machine (UTM) (Model: H 75 KS) at a strain rate of 0.003/second. The variation of UTS and YS at fracture and the percentage elongation concerning TiO_2 content is shown in Table 2. The un-reinforced AA2014 has lower strength and higher elongation when compared to the developed composites. The composites have achieved good work hardening capacity that shows significant plastic strain before fracture to a fair extent. The developed composite with 4 wt% of TiO_2 is found to exhibit maximum strength with a UTS of 328 MPa and a YS of 312 MPa which are 41.2% and 34.1% higher compared to the un-reinforced AA2014, respectively. The incorporation of TiO_2 ceramic particles has strengthened the composites due to their hard nature compared to the base alloy. The reinforcement has imparted additional strength to the composites due to direct and indirect strengthening mechanisms. Direct strengthening is based on the good interfacial bonding between matrix and reinforcement which directly affects the transfer of load.[34] Further, the wetting angle between the matrix and reinforcement, presence of pores, microcracks and microvoids are the functions of interfacial bonding.[53] In the present study, the uniform distribution of the hard particles can be seen as a parameter that directly influences the tensile strength of composites.

Indirect strengthening is mainly focused on the effect of reinforcement on the matrix phase. The improvement of strength in the developed composites can be attributed to the following strengthening mechanisms: (1) The dispersion strengthening provided by TiO_2 particles and the Al_2O_3 formed in the matrix,[54] (2) Grain refinement,[55] (3) Additional strength provided by the secondary intermetallic phases in the matrix[56] (4) Strain-induced between the matrix and reinforcement,[54,57] etc. Generally, these mechanisms act in combination with each other. As discussed earlier, due to the presence of dispersed particles in the matrix, when a load is applied to the material, the dislocations move and form dislocation loops or bows around the particle which acts as a barrier to their movement and results in enhancing the strength. Next, grain refinement leads to smaller grains and more grain boundaries restrict the motion of dislocation according to Hall-Petch theory. Besides, the thermal mismatch in the matrix due to the difference in thermal coefficients generates a strain field

around the particles during solidification. These strain fields cause hindrance to the dislocation movement at the interface and thus increases the yield strength.[58] The main strengthening mechanism in the present composite is provided by phases such as Al_2Cu and Al_2CuMg.[59] From Figure 5, it is observed that both these phases become coarser and the Al_2O_3 TiO_2 particles tend to agglomerate after 3 wt% TiO_2 addition. The harder Al_2O_3 also act as particles along with TiO_2 and further increases the strength. The results of the mechanical properties showed that the composite with 4 wt% TiO_2 exhibited the highest values of hardness, UTS and YS. But, it is important to note that the difference in the properties between 3 wt% and 4 wt% reinforced composites is very less. It seems that the properties more or less tend to saturate after 3 wt% TiO_2 addition. However, Table 2 shows that beyond 3 wt% TiO_2 addition, the elongation falls steeply. The presence of hard particles offers resistance to plastic deformation and increases the strength but decreases the % elongation of the developed composite at the same time when added beyond a point.[21]

Compressive Strength

Three cylindrical samples from each composite were prepared for compression testing according to ASTM standards E9-09 standards to evaluate the compression strength of the developed composites. The testing is done by a universal Testing Machine (UTM) (Model: H 75 KS) at a strain rate of 0.003/second. The variation in the compressive strength from each composite with an increase in the TiO_2 content is shown in Table 2.

As the wt% of reinforcement particles increases, there is an increasing trend in the compressive strength of the composites. The developed composite with 4 wt% of TiO_2 shows a maximum of 793 MPa strength which is a 59.5% increase when compared to the base alloy. The compressive strength of composite samples can also be attributed mainly to the mechanisms discussed above. Substantial grain refinement, dislocation interaction due to elastic modulus mismatch, load transfer from matrix to reinforcement and other phases formed in the matrix contribute to the increase in the compressive strength of the composites.[60,61]

Conclusions

In the present work, AA2014-TiO_2 composites are successfully developed through a multi-step stir casting method. Based on the investigations made on the microstructural and mechanical properties and their corresponding results, the following conclusions are drawn.

- The multi-step stirring promoted the formation of in situ Al_2O_3 formation in the matrix and uniform distribution of TiO_2 particles and enhances the interfacial bonding that is not much attainable through conventional stirring as seen from Figure 4 (e). The as-cast microstructure consists of α-Al dendrite structure with eutectic phases which were separated by adding TiO_2 particles. Phases such as Al_2Cu, Al_2CuMg and Al_2O_3 were found in eutectic phases providing additional strength to the composites as confirmed by XRD and EDX.
- The microstructure in Figures 4 and 5 reveals that grain refinement is achieved with the addition of TiO_2, and the refinement increases up to 3 wt% of TiO_2 addition after which it saturates. The main strengthening mechanisms are found to be dispersion strengthening, secondary phase and grain boundary strengthening. The grain sizes of the composite samples calculated from the microstructures are 124, 46, 43, 32, 30 μm, respectively. No remarkable refinement was observed beyond 3 wt% TiO_2 addition.
- In the matrix, the secondary Al_2Cu phase, intermetallic Al_2CuMg phase and the formed Al_2O_3 increase with an increase in the TiO_2 addition which controlled the trend of change in the properties. The harder Al_2O_3 also act as particles along with TiO_2 and further increases the strength. Beyond 3 wt% TiO_2 addition, the phases coarsen around the grain boundaries and the properties tend to saturate.
- It is found that the hardness, tensile strength and compressive strength of composite samples increase with an increase in the wt% of TiO_2 particles. However, there was no notable improvement in the properties of the composite beyond 3 wt% TiO_2 addition. Moreover, with the addition of TiO_2, the % elongation decreased, particularly when added beyond 3 wt%.
- The composite sample with 4 wt% TiO_2 showed the highest mechanical properties like 91.1 Hv of hardness, 318 MPa of UTS and 302 MPa of YS, respectively, which are 60%, 86% 111% higher compared to that of the base alloy.

Acknowledgment

The authors would like to thank The Mechanical Industrial Department of IIT Roorkee for providing the necessary equipment required for this study.

Funding

The first author would like to thank MHRD, Govt. of India for providing fellowship.

Availability of data material

Data will be made available on request to the corresponding author.

Code Availability

No code is used.

Conflict of interest The authors declare no conflicts of interest whatsoever.

REFERENCES

1. V.P. Baisane, Y.S. Sable, M.M. Dhobe, P.M. Sonawane, A. Sicp, Recent development and challenges in processing of ceramics reinforced Al matrix composite through stir casting process: a review. int. J. Eng. Appl. Sci. **2**, 11–16 (2015)
2. G. Moona, R.S. Walia, V. Rastogi, R. Sharma, Aluminium metal matrix composites: a retrospective investigation. Indian J. Pure Appl. Phys. **56**, 164–175 (2018)
3. R.T. Holt, A.K. Koul, L. Zhao, W. Wallace, J.C. Beddoes, Lightweight materials for aircraft applications. Mater. Charact. **67**, 41–67 (1995)
4. T. Dursun, C. Soutis, Recent developments in advanced aircraft aluminium alloys. Mater. Des. **56**, 862–871 (2014). https://doi.org/10.1016/j.matdes.2013.12.002
5. C.S. Jawalkar, S. Kant, A review on use of aluminium alloys in aircraft components, I-Manager's. J. Mater. Sci. **3**, 33–38 (2018). https://doi.org/10.26634/jms.3.3.3673
6. M.K. Surappa, Aluminium matrix composites: challenges and opportunities. Sadhana **28**, 319–334 (2003)
7. K.N. Braszczyńska-Malik, E. Przełożyńska, The influence of Ti particles on microstructure and mechanical properties of Mg-5Al-5RE matrix alloy composite. J. Alloys Compd. **728**, 600–606 (2017). https://doi.org/10.1016/j.jallcom.2017.08.177
8. C.H.S. Vidyasagar, D.B. Karunakar, Effects of nano yttrium and spark plasma sintering on the mechanical properties of AA2024 matrix composites. Met. Mater. Int. (2020). https://doi.org/10.1007/s12540-020-00727-4
9. C.H.S. Vidyasagar, D.B. Karunakar, Effects of yttrium addition and aging on mechanical properties of AA2024 fabricated through multi-step stir casting. Trans. Nonferrous Met. Soc. China (English Ed.) **30**, 288–302 (2020). https://doi.org/10.1016/S1003-6326(20)65213-X
10. C.H.S. Vidyasagar, D.B. Karunakar, Characterization of mechanical properties and microstructures of spark plasma sintered and cryo-rolled AA2024-Y composites. Trans. Nonferrous Met. Soc. China (English Ed.) **30**, 1439–1451 (2020). https://doi.org/10.1016/S1003-6326(20)65309-2
11. K. Almadhoni, S. Khan, Review of effective parameters of stir casting process on metallurgical properties of ceramics particulate Al composites ceram. Part. Al Compos. **6**, 21–40 (2016). https://doi.org/10.9790/1684-12642240
12. M. Rashad, F. Pan, Y. Liu, X. Chen, H. Lin, R. Pan, M. Asif, J. She, High temperature formability of graphene nanoplatelets-AZ31 composites fabricated by stir-casting method. J. Magnes. Alloy. **4**, 270–277 (2016). https://doi.org/10.1016/j.jma.2016.11.003
13. H. Hanizam, M.S. Salleh, M.Z. Omar, A.B. Sulong, Optimisation of mechanical stir casting parameters for fabrication of carbon nanotubes-aluminium alloy composite through Taguchi method. J. Mater. Res. Technol. **8**, 2223–2231 (2019). https://doi.org/10.1016/j.jmrt.2019.02.008
14. J.A.T. Sudipt Kumar, Metal matrix composite production and characterisation of aluminium-fly ash composite using stir casting method production and characterisation of aluminium-fly ash composite using stir casting method. Mater. Eng. (2008) 1–57.
15. A.K.M.A. Iqbal, D.M. Nuruzzaman, Effect of the reinforcement on the mechanical properties of aluminium matrix composite: a review. Nanomaterials **11**, 10408–10413 (2016)
16. P. Dev, M.S. Charoo, Role of reinforcements on the mechanical and tribological behavior of aluminum metal matrix composites: a review. Mater. Today Proc. **5**, 20041–20053 (2018). https://doi.org/10.1016/j.matpr.2018.06.371
17. C.S. Vidyasagar, D.B. Karunakar, Improvement of mechanical properties of 2024 AA by reinforcing yttrium and processing through spark plasma sintering. Arab. J. Sci. Eng. **44**(2019), 7859–7873 (2019). https://doi.org/10.1007/s13369-019-03924-5
18. R. Zamani, H. Mirzadeh, M. Emamy, Mechanical properties of a hot deformed Al-Mg2Si in-situ composite. Mater. Sci. Eng. A. **726**, 10–17 (2018). https://doi.org/10.1016/j.msea.2018.04.064
19. V.S. Ayar, M.P. Sutaria, Development and characterization of in situ AlSi5Cu3/TiB2 composites. Int. J. Met. **14**, 59–68 (2020). https://doi.org/10.1007/s40962-019-00328-x
20. P. Senthil Kumar, V. Kavimani, K. Soorya Prakash, V. Murali Krishna, G. Shanthos-Kumar, Effect of TiB2 on the corrosion resistance behaviour of in situ Al composites. Int. J. Met. **14**, 84–91 (2020). https://doi.org/10.1007/s40962-019-00330-3
21. K. Ravi-Kumar, K. Kiran, V.S. Sreebalaji, Micro structural characteristics and mechanical behaviour of aluminium matrix composites reinforced with titanium carbide. J. Alloys Compd. **723**, 795–801 (2017). https://doi.org/10.1016/j.jallcom.2017.06.309
22. R.H. Oskouei, R.N. Ibrahim, An investigation on the fatigue behaviour of Al 7075–T6 coated with titanium nitride using physical vapour deposition process.

Mater. Des. **39**, 294–302 (2012). https://doi.org/10.1016/j.matdes.2012.02.056
23. C.S. Vidyasagar, D.B. Karunakar, Effect of spark plasma sintering and reinforcements on the formation of ultra-fine and nanograins in AA2024-TiB2-Y hybrid composites. Prog. Nat. Sci. Mater. Int. (2021). https://doi.org/10.1016/j.pnsc.2021.07.001
24. P.M. Ashraf, L. Edwin, Corrosion behaviour of nanometre sized cerium oxide and titanium oxide incorporated aluminium in NaCl solution. J. Alloys Compd. **548**, 82–88 (2013). https://doi.org/10.1016/j.jallcom.2012.09.020
25. S.V. Alagarsamy, M. Ravichandran, Synthesis, microstructure and properties of TiO2 reinforced AA7075 matrix composites via stir casting route. Mater. Res. Express. (2019). https://doi.org/10.1088/2053-1591/ab1d3b
26. J.H. Shin, H.J. Choi, D.H. Bae, The structure and properties of 2024 aluminum composites reinforced with TiO2 nanoparticles. Mater. Sci. Eng. A. **607**(2014), 605–610 (2014). https://doi.org/10.1016/j.msea.2014.04.038
27. I. Dutta, C.P. Harper, G. Dutta, Role of Al2O3 particulate reinforcements on precipitation in 2014 Al-matrix composites. Metall. Mater. Trans. A. **25**(1994), 1591–1602 (1994). https://doi.org/10.1007/BF02668525
28. S. Siddesha, Effects of fabrication of aluminium 2024/Tio2 metal matrix composite. Int. J. Innov. Res. Dev. **5**, 174–177 (2016)
29. M. Nagaral, V. Hiremath, V. Auradi, S.A. Kori, Influence of two-stage stir casting process on mechanical characterization and wear behavior of AA2014-ZrO2 Nano-composites. Trans. Indian Inst. Met. **71**, 2845–2850 (2018). https://doi.org/10.1007/s12666-018-1441-6
30. K. Prapasajchavet, Y. Harada, S. Kumai, Microstructure analysis of Al-5.5 at%Mg alloy semi-solid slurry by weck's reagent. Int. J. Met. **11**, 123–130 (2017). https://doi.org/10.1007/s40962-016-0084-9
31. U. Aybarc, O. Ertuğrul, M.Ö. Seydibeyoğlu, Effect of Al2O3 particle size on mechanical properties of ultrasonic-assisted stir-casted Al A356 matrix composites. Int. J. Met. **15**, 638–649 (2021). https://doi.org/10.1007/s40962-020-00490-7
32. P. Ashtari, G. Birsan, A. Khalaf, S. Shankar, Technical development report controlled diffusion solidification of 2024, 6082 and 7075 Al alloys via tilt-pour casting process. Int. J. Met. **5**, 43–64 (2011). https://doi.org/10.1007/BF03355471
33. S.P. Midson, A. Jackson, A comparison of thixocasting and rheocasting, Inst. Cast Met. Eng. - 67th World Foundry Congr. Wfc06 Cast. Futur. 2 (2006) 1081–1090.
34. B. Zhou, S. Lu, K. Xu, C. Xu, Z. Wang, Microstructure and simulation of semisolid aluminum alloy castings in the process of stirring integrated transfer-heat (SIT) with water cooling. Int. J. Met. **14**, 396–408 (2020). https://doi.org/10.1007/s40962-019-00357-6
35. N. Nayan, A. Agarwal, G. Bajargan, A.K. Jha, P.R. Narayanan, K. Sreekumar, M.C. Mittal, A study of continuously cast ingots of aluminum alloy aa2014 with increased ultrasonic characteristics. Met. Sci. Heat Treat. **53**, 363–368 (2011). https://doi.org/10.1007/s11041-011-9399-6
36. C. HariKrishna, M.J. Davidson, Damage modeling and critical damage evaluation of AA2014 cast alloy embedded with fly ash composite under upsetting. Proc. Inst. Mech. Eng. Part C J. Mech. Eng. Sci. 233 (2019) 5227–5236. doi:https://doi.org/10.1177/0954406219844285.
37. R.D. Manikonda, M.B.S. Sreekara Reddy, K. Arul Raj, Wear characteristics investigations of AA2014-SiC under dry sliding conditions. J. Crit. Rev. **7**, 824–831 (2020). https://doi.org/10.31838/jcr.07.09.155
38. C.S. Vidyasagar, D.B. Karunakar, Effects of yttrium addition and aging on mechanical properties of AA2024 fabricated through multi-step stir casting. Trans. Nonferrous Met. Soc. China. **30**, 288–302 (2020). https://doi.org/10.1016/S1003-6326(20)65213-X
39. J.S. Khalkho, C.H.S. Vidyasagar, D.B. Karunakar, Evaluation of microstructure and mechanical properties of Al-tac composites developed by multi-step stir casting process, ASME 2020 15th Int. Manuf. Sci. Eng. Conf. MSEC 2020. 1 (2020) 1–9. doi:https://doi.org/10.1115/MSEC2020-8291
40. J. Rogal, H.V. Dutkiewicz, L. Atkinson, T. Lityńska-Dobrzyńska, M. Czeppe, Modigell, Characterization of semi-solid processing of aluminium alloy 7075 with Sc and Zr additions. Mater. Sci. Eng. A. **580**, 362–373 (2013). https://doi.org/10.1016/j.msea.2013.04.078
41. S.K. Pradhan, S. Chatterjee, A.B. Mallick, D. Das, A simple stir casting technique for the preparation of in situ Fe-aluminides reinforced Al-matrix composites. Perspect. Sci. **8**, 529–532 (2016). https://doi.org/10.1016/j.pisc.2016.06.011
42. A. Veillère, H. Kurita, A. Kawasaki, Y. Lu, J.M. Heintz, J.F. Silvain, Aluminum/carbon composites materials fabricated by the powder metallurgy process. Materials (Basel). **12**, 1–15 (2019). https://doi.org/10.3390/ma1224030
43. Y. Sun, C. Zhang, L. He, Q. Meng, B.C. Liu, K. Gao, J. Wu, Enhanced bending strength and thermal conductivity in diamond/Al composites with B4C coating. Sci. Rep. **8**, 1–12 (2018). https://doi.org/10.1038/s41598-018-29510-7
44. K.K. Alaneme, A.O. Aluko, Production and age-hardening behaviour of borax premixed SiC reinforced Al-Mg-Si alloy composites developed by double stir-casting technique. West Indian J. Eng. **34**, 80–85 (2012)

45. K.K. Alaneme, A.O. Aluko, Fracture toughness (K 1C) and tensile properties of as-cast and age-hardened aluminium (6063)silicon carbide particulate composites. Sci. Iran. **19**, 992–996 (2012). https://doi.org/10.1016/j.scient.2012.06.001
46. C. Mallikarjuna, S.M. Shashidhara, U.S. Mallik, K.I. Parashivamurthy, Grain refinement and wear properties evaluation of aluminum alloy 2014 matrix-TiB2 in-situ composites. Mater. Des. **32**, 3554–3559 (2011). https://doi.org/10.1016/j.matdes.2011.01.036
47. J. David Raja Selvam, I. Dinaharan, S. Vibin Philip, P.M. Mashinini, Microstructure and mechanical characterization of in situ synthesized AA6061/(TiB2+Al2O3) hybrid aluminum matrix composites. J. Alloys Compd. **740**, 529–535 (2018). https://doi.org/10.1016/j.jallcom.2018.01.016
48. J. Grilo, V.H. Carneiro, J.C. Teixeira, H. Puga, Manufacturing methodology on casting-based aluminium matrix composites: systematic review. Metals (Basel). **11**, 1–30 (2021). https://doi.org/10.3390/met11030436
49. S. Aravindan, P.V. Rao, K. Ponappa, Evaluation of physical and mechanical properties of AZ91D/SiC composites by two step stir casting process. J. Magnes. Alloy. **3**, 52–62 (2015). https://doi.org/10.1016/j.jma.2014.12.008
50. R. Gupta, G.P. Chaudhari, B.S.S. Daniel, Strengthening mechanisms in ultrasonically processed aluminium matrix composite with in-situ Al3Ti by salt addition. Compos. Part B Eng. **140**, 27–34 (2018). https://doi.org/10.1016/j.compositesb.2017.12.005
51. R.G. Guan, Z.Y. Zhao, R.Z. Chao, Z.X. Feng, C.M. Liu, Microstructure evolution and solidification behaviors of A2017 alloy during cooling/stirring and rolling process. Trans. Nonferrous Met. Soc. China (English Ed.) **22**, 2871–2876 (2012). https://doi.org/10.1016/S1003-6326(11)61544-6
52. H. Queudet, S. Lemonnier, E. Barraud, J. Guyon, J. Ghanbaja, N. Allain, E. Gaffet, One-step consolidation and precipitation hardening of an ultrafine-grained Al-Zn-Mg alloy powder by Spark Plasma Sintering. Mater. Sci. Eng. A. **685**, 227–234 (2017). https://doi.org/10.1016/j.msea.2017.01.009
53. G. Chen, X. Song, N. Hu, H. Wang, Y. Tian, Effect of initial Ti powders size on the microstructures and mechanical properties of Al3Ti/2024 Al composites prepared by ultrasonic assisted in-situ casting. J. Alloys Compd. **694**, 539–548 (2017). https://doi.org/10.1016/j.jallcom.2016.10.039
54. J.B. Ferguson, B.F. Schultz, D. Venugopalan, H.F. Lopez, P.K. Rohatgi, K. Cho, C.S. Kim, On the superposition of strengthening mechanisms in dispersion strengthened alloys and metal-matrix nanocomposites: Considerations of stress and energy. Met. Mater. Int. **20**, 375–388 (2014). https://doi.org/10.1007/s12540-014-2017-6
55. R.G. Guan, D. Tie, A review on grain refinement of aluminum alloys: Progresses, challenges and prospects. Acta Metall. Sin. (English Lett.) **30**, 409–432 (2017). https://doi.org/10.1007/s40195-017-0565-8
56. A. Staszczyk, J. Sawicki, B. Adamczyk-Cieslak, A study of second-phase precipitates and dispersoid particles in 2024 aluminum alloy after different aging treatments. Materials (Basel). (2019). https://doi.org/10.3390/ma1224168
57. J. Jiang, Y. Liu, G. Xiao, Y. Wang, Y. Ju, Effect of pass reduction on microstructure, mechanical properties and texture of hot-rolled 7075 alloy. Mater. Charact. **147**, 324–339 (2019). https://doi.org/10.1016/j.matchar.2018.11.015
58. J.A.K. Gladston, N.M. Sheriff, I. Dinaharan, J.D. Raja-Selvam, Production and characterization of rich husk ash particulate reinforced AA6061 aluminum alloy composites by compocasting. Trans. Nonferrous Met. Soc. China **25**, 683–691 (2015). https://doi.org/10.1016/S1003-6326(15)63653-6
59. G.M.N. Nowotnik, J. Sieniawski, Analysis of intermetallic phases in 2024 aluminium alloy. Solid State Phenom. **197**, 238–243 (2013). https://doi.org/10.4028/www.scientific.net/SSP.197.238
60. A. Patel, S. Das, B.K. Prasad, Compressive deformation behaviour of Al alloy (2014)-10wt% SiCp composite: effects of strain rates and temperatures. Mater. Sci. Eng. A. **530**, 225–232 (2011). https://doi.org/10.1016/j.msea.2011.09.078
61. S.A. Sajjadi, H.R. Ezatpour, M. Torabi-Parizi, Comparison of microstructure and mechanical properties of A356 aluminum alloy/Al2O3 composites fabricated by stir and compo-casting processes. Mater. Des. **34**, 106–111 (2012). https://doi.org/10.1016/j.matdes.2011.07.037